

A Dynamic Measurement Technique for Third-Order Distortion in Optical Phase Modulators

Matthew N. Sysak, *Member, IEEE*, Leif Johansson, *Member, IEEE*, Jonathan S. Klamkin, *Student Member, IEEE*, Larry A. Coldren, *Fellow, IEEE*, and John E. Bowers, *Fellow, IEEE*

Abstract—A novel two-tone measurement technique for characterizing distortion in optical phase modulators is proposed and demonstrated. The technique is used to characterize an InGaAsP–InP modulator in a monolithically integrated receiver. Results for forward and reverse bias conditions in the modulator show a phase IP3 of 7.2π and 0.97π rad, respectively.

Index Terms—Carrier injection, phase distortion, phase modulators, quantum confined stark effect.

I. INTRODUCTION

TRANSMISSION systems that utilize optical phase modulation are attractive for both analog and digital communication links. In analog transmission applications, phase modulation is attractive since it is not limited by the zero and full rail levels in standard intensity modulated systems. For digital transmission links, phase modulated systems provide tolerance to fiber dispersion effects and wide wavelength transparency.

To evaluate the performance of various phase modulators, several characterization techniques have been employed. For static characterization, phase efficiency experiments can be performed using shifts in a Fabry–Pérot cavity or by utilizing a Mach–Zehnder interferometer (MZI) [1], [2]. However, dynamic distortion characterization of phase modulators has been limited to single tone measurements because nonlinearities in the phase detection process are difficult to separate from the nonlinearities produced by the modulator [3].

In this work, we propose and demonstrate a two-tone measurement technique for characterizing the distortion generated by optical phase modulators that is not limited by the distortion in the phase recovery process. The technique relies on a linear external LiNbO₃ phase modulator to cancel the fundamental response of the test modulator, keeping the phase to amplitude phase recovery process within the linear regime of an optical MZI. Cancellation of the fundamental response does not effect the third-order distortion terms. Using this technique, we have compared the linearity of an InGaAsP phase modulator under forward and reverse bias conditions that is part of an integrated InGaAsP–InP photonic receiver chip. The comparisons are based on a modulator phase third-order intercept point (IP3), where the distortion and fundamental phase response of the test device are equivalent.

Manuscript received July 26, 2006; revised November 9, 2006. This work was supported by Defense Advanced Research Projects Agency (DARPA)/MTO Phorfront under Grant N66001-02-C-8026.

The authors are with the Department of Electrical Engineering and the Department of Materials, University of California Santa Barbara, Santa Barbara, CA 93116 USA (e-mail: mnsysak@engineering.ucsb.edu).

Digital Object Identifier 10.1109/LPT.2006.890026

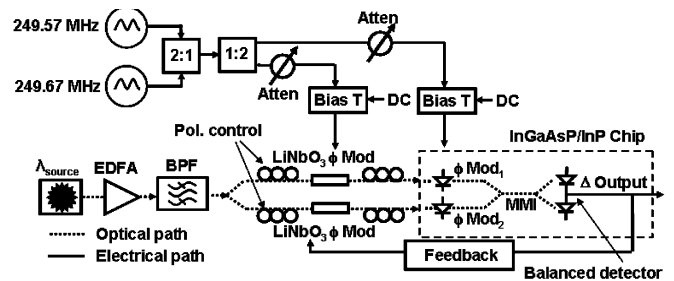


Fig. 1. Experimental setup for the dynamic characterization of third-order distortion products in InGaAsP phase modulators. Optical paths are denoted by dashed lines and electrical paths are shown as solid lines.

II. EXPERIMENTAL SETUP

The experimental setup used in these measurements is shown in Fig. 1. The setup is divided into electrical and optical sections. The optical portion consists of an optical transmitter, including a laser source at 1550 nm, an erbium-doped fiber amplifier, and an optical filter, that is split into two arms of an MZI and then recombined in a balanced photodetector (PD). Both arms of the MZI contain an external LiNbO₃ modulator and a 500- μm -long InGaAsP phase modulator that is part of the photonic receiver chip. Polarization controllers are utilized before and after each LiNbO₃ modulator. The photonic chip contains two parallel waveguides, each with an integrated InGaAsP phase modulator, a 2×2 multimode interference combiner, and a set of 100- μm -long uni-traveling-carrier (UTC)-PDs placed in a balanced configuration [4]. The InGaAsP phase modulator (ϕ mod₂) in the lower arm of the MZI is used to bias the interferometer. The InGaAsP modulators utilize 7×6.5 nm quantum wells and 6×5 nm barriers with a photoluminescence peak of 1465 nm centered in an optical waveguide layer for phase efficiency.

The electrical portion of the test setup consists of two signal generators and a series of electrical splitters and combiners. The individual tones from each function generator are combined in a 2 : 1 combiner, then split into two electrical paths using a 1 : 2 splitter. The outputs from the splitter contain signal tones from both function generators. One of the outputs from the splitter is routed to the LiNbO₃ modulator, while the second output is routed to the test modulator (ϕ mod₁). A set of attenuators are used to control the electrical power delivered to the modulators. A portion of the signal from the balanced detector is routed to a low frequency feedback circuit. The output from the circuit is connected to a second LiNbO₃ modulator, which compensates low frequency drift in the test bed and forces the power difference at the output of the balanced detector to zero [5]. To

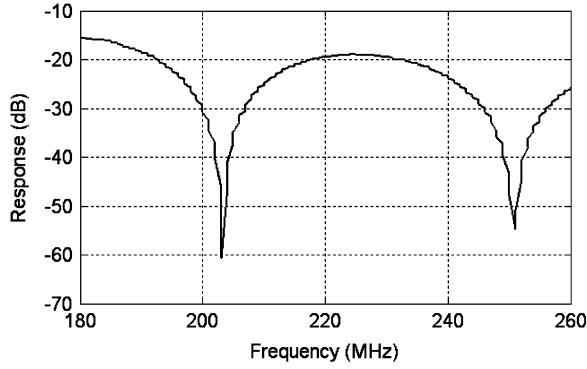


Fig. 2. Frequency response measurements between the 1 : 2 splitter and the balanced UTC-PD. Nulls correspond to frequencies where the path length mismatches between the LiNbO₃ and InGaAsP modulators are separated by an odd multiple of π radians.

ensure that the nonlinearities associated with the test equipment and the various splitters and combiners in the test bed are minimized, the two-tone electrical signal used to drive the LiNbO₃ and InGaAsP modulators was examined over a range of electrical powers. The drive signals contained no observable distortion for power levels up to and exceeding the levels utilized in our experiments. To eliminate the possibility that distortion might be generated in the UTC-PDs, two-tone measurements were performed on a set of test devices with the same dimensions as the photodiodes in the receiver chip. Results showed an output power IP₃ of $> +30$ dBm for the $100 \times 10 \mu\text{m}^2$ UTC-PD at a bias of -5 V [4].

The center frequency of the two-tone signal is chosen so that the path length difference between the 1 : 2 electrical splitter and the InGaAsP or LiNbO₃ modulator corresponds to a phase delay of an odd multiple of π radians. To investigate the electrical delay between the two paths, the function generators and the 2 : 1 combiner were removed and a frequency response measurement was performed between the 1 : 2 splitter and the balanced UTC-PD. Results from this measurement are shown in Fig. 2 when the InGaAsP modulator is forward biased. Dips in the response correspond to frequencies where the electrical path lengths are mismatched by an odd multiple of π radians. Under these conditions, the 180° phase lag between the signals to each modulator cause the phase response of the two devices to cancel. The roll off of the response in this measurement is a result of a low (~ 150 MHz) 3-dB bandwidth of the forward biased InGaAsP modulator [2].

III. MEASUREMENT TECHNIQUE

Characterization of the reverse and forward bias InGaAsP phase modulator requires a set of two experiments. All measurements are performed at an MZI bias where the average photocurrent in both UTC-PDs is 1.7 mA.

The first set of experiments examines the fundamental response of the test modulator. This experiment uses only the test InGaAsP modulator and does not utilize the LiNbO₃ modulator. The bias-T in the electrical path sets either forward or reverse bias conditions in the device. In this experiment, the power from the two electrical signal generators that is routed to the test device is varied and the fundamental and third-order signal tones from the balanced UTC-PD are measured in a $50\text{-}\Omega$

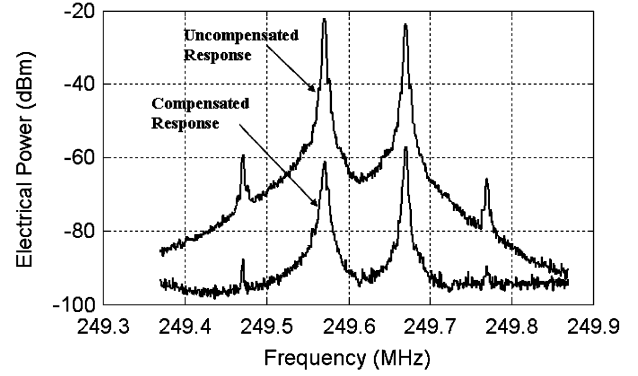


Fig. 3. Compensated and uncompensated spectra for forward biased InGaAsP phase modulator. Electrical drive power is -15 and 0 dBm to the InGaAsP and LiNbO₃ modulators, respectively. The compensated spectra has not been optimized for maximum distortion suppression.

terminated electrical spectrum analyzer (ESA). Although the distortion measured at the output of the balanced detector has components associated with both the modulator and the optical MZI, the fundamental phase response of the InGaAsP modulator remains proportional to the fundamental tone produced in the balanced detector. An output spectrum from these experiments with the forward biased modulator is shown in Fig. 3. The spectrum is labeled “Uncompensated Response.”

The second set of experiments utilizes both modulators and is used to extract the InGaAsP modulator distortion. In these measurements, the electrical power to the test and reference modulators is varied and the output from the balanced UTC-PD is examined in an ESA. The phase difference between the electrical signals to the two modulators causes the phase response of the LiNbO₃ modulator to compensate the phase response of the InGaAsP device. Since the LiNbO₃ modulator relies on the linear electrooptic effect and the forward or reverse biased InGaAsP modulator relies on the highly nonlinear quantum confined stark effect and plasma effect, the phase cancellation between these modulators affects primarily the fundamental response of the InGaAsP device while the preserving modulator distortion products. The reduced fundamental permits the phase-to-amplitude conversion to remain in the linear regime of the MZI, preserving the distortion produced in the test modulator without adding distortion from the phase recovery process. A sample spectrum from the UTC-PDs in these experiments is shown in Fig. 3 and labeled “Compensated Response.”

IV. RESULTS

Results for characterization of the forward biased InGaAsP modulator with a 10-mA DC bias are shown in Fig. 4.

In the uncompensated measurements, Fig. 4 shows an input power IP₃ of $+7.6$ dBm. Using a modulator V_π of 0.5 V, this translates into a peak phase IP₃ of 1.5π rad. The phase IP₃ can also be calculated based on the output power IP₃ in Fig. 4. Based on the phase efficiency of 3.4 mA/rad in the balanced detector, this translates into a peak phase IP₃ of 0.45π rad. Both results are in relatively good agreement with the 0.9π peak phase limit that is associated with an optical MZI [6]. It should be noted that any RF losses at the detector or any deviation from the quadrature point in the test setup caused by imbalance coupler splitting

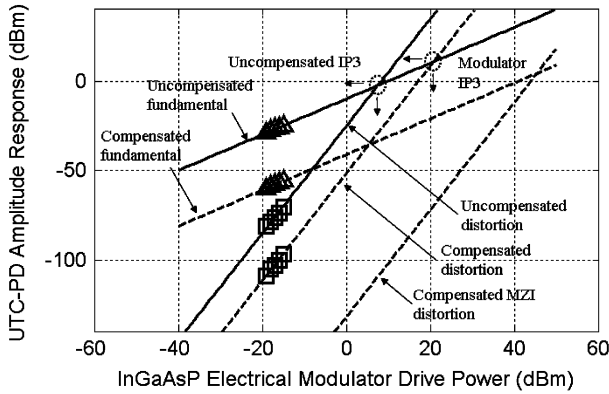


Fig. 4. Uncompensated and compensated experimental results generated by the forward biased InGaAsP phase modulator.

reduces the output power IP3 in these measurements and would cause an artificially low phase IP3.

For the compensated measurements, the cancellation of the InGaAsP fundamental by ~ 33 dB leads to a suppression of the MZI nonlinearities and isolation of the modulator distortion. The corresponding reduction of the measured distortion is ~ 33 dB. It is important that although the fundamental phase response is reduced, it is not eliminated, and the compensated measurements are still limited by the theoretical phase IP3 of 0.9π associated with the MZI. The theoretical distortion generated by the test setup is included in Fig. 4 and labeled “compensated MZI distortion.” The experimental data in these measurements is >20 dB above the theoretical MZI distortion, indicating that the test bed nonlinearities have been sufficiently removed to expose the modulator distortion.

Combining the fundamental response in the uncompensated measurements with the third-order response in the compensated measurements allows extraction of the forward biased modulator phase characteristics. From Fig. 4, the input power IP3 is $+20.9$ dBm, which corresponds to a phase IP3 of 7.2π . As mentioned previously, the output power IP3 can also be used to calculate phase IP3. The $+10.85$ -dBm output power IP3 in Fig. 4 corresponds to a phase IP3 of 2.1π rad. However, the most accurate measure of the modulator performance is most likely the calculation of phase IP3 based on the input power. This is because the UTC-PD losses and MZI imbalance or bias offsets from quadrature reduce the RF power from the detector and make the phase IP3 appear artificially small.

Results for the reverse biased modulator characterization are shown in Fig. 5. The applied DC bias is -2 V. Examining the distortion and fundamental tones in the uncompensated measurements shows an output and input power IP3 of -7.2 and $+24.7$ dBm, respectively. Converting this to an output phase change gives 0.8π rad based input power IP3 ($V\pi$ is 6.8 V) and 0.25π rad based on the output power IP3. The phase IP3 based on the input power IP3 is in good agreement with the 0.9π that should limit the MZI, and indicates that the modulator distortion is roughly equal to the distortion generated by the test setup.

In the compensated measurements when the test bed nonlinearities are reduced, the very small (~ 3 – 4 dB) reduction in the distortion data supports the conclusion that the modulator and

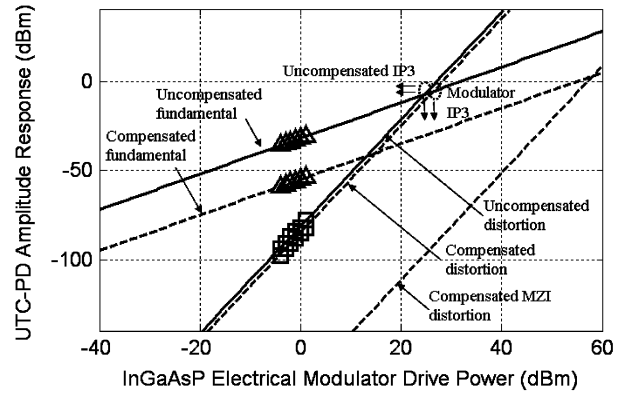


Fig. 5. Uncompensated and compensated experimental results generated by the reverse biased InGaAsP phase modulator.

test bed distortion are roughly equivalent. As in Fig. 4, the distortion associated with the MZI in the compensated measurements is included in Fig. 5, and is labeled “compensated MZI distortion.”

Extrapolating the fundamental response from the uncompensated measurements and the distortion in the compensated measurements gives input and output power IP3s $+26.4$ and -5.65 dBm, respectively. Converting the input power power IP3s to phase gives a phase IP3 for the reverse biased modulator of 0.97π rad.

V. CONCLUSION

We have proposed and demonstrated a dynamic measurement technique for characterizing distortion products in optical phase modulators. The technique has been used to characterize the nonlinearities in an InGaAsP phase modulator under forward and reverse bias conditions. Measurements of the test modulator under forward and reverse bias conditions showed a phase IP3 of $\sim 7.2\pi$ and 0.97π , respectively.

REFERENCES

- [1] H. Mohseni, H. An, Z. A. Shellenbarger, M. H. Kwakernaak, A. N. Lepore, J. H. Abeles, and P. J. Delfyett, “Highly linear and efficient GaInAsP-InP phase modulators,” in *Conf. Lasers Electro-Optics (LEOS)*, 2004, vol. 1, p. 2.
- [2] M. N. Sysak, L. A. Johansson, J. W. Raring, M. Rodwell, L. A. Coldren, and J. E. Bowers, “A high-efficiency, current injection based quantum well phase modulator monolithically integrated with a tunable laser for coherent systems,” in *Coherent Optical Technol. and Appl. (COTA) CFC6*, Whistler, BC, Canada, Jun. 2006.
- [3] R. E. Tench, J. M. P. Delavaux, L. D. Tzeng, R. W. Smith, L. L. Buhl, and R. C. Alferness, “Performance evaluation of waveguide phase modulators for coherent systems at 1.3 and 1.5 μm ,” *J. Lightw. Technol.*, vol. LT-5, no. 4, pp. 492–501, Apr. 1987.
- [4] J. Klamkin, L. A. Johansson, A. Ramaswamy, H. F. Chou, M. N. Sysak, J. W. Raring, N. Parthasarathy, S. P. Denbaars, J. E. Bowers, and L. A. Coldren, “Monolithically integrated balanced uni-travelling-carrier photodiode with tunable MMI coupler for microwave photonic circuits,” *COMMAD*, 2006, submitted for publication.
- [5] H. F. Chou, D. Zibar, L. A. Johansson, and J. E. Bowers, “SFDR Improvement of a Coherent Receiver Using Feedback,” in *Coherent Optical Technol. and Appl. (COTA) CFA3*, Whistler, BC, Canada, Jun. 2006.
- [6] B. Kolner and D. W. Dolfi, “Intermodulation Distortion and compression in an Integrated Electrooptic Modulator,” *Appl. Opt.*, vol. 26, no. 2, pp. 3676–3680, Sep. 1987.